



## Buffalo weed (*Ambrosia trifida* L. var. *trifida*) biochar for cadmium (II) and lead (II) adsorption in single and mixed system

Kalyan Yakkala<sup>a</sup>, Mok-Ryun Yu<sup>a</sup>, Hoon Roh<sup>a</sup>, Jae-Kyu Yang<sup>b</sup>, Yoon-Young Chang<sup>a,\*</sup>

<sup>a</sup>Department of Environmental Engineering, Kwangwoon University, Seoul 139-701, Korea  
Tel. +82 2 940 5496; Fax: +82 2 918 5774; email: yychang@kw.ac.kr

<sup>b</sup>Division of General Education, Kwangwoon University, Seoul 139-701, Korea

Received 15 May 2012; Accepted 6 March 2013

### ABSTRACT

Biochars (BWBC 300, BWBC 500 and BWBC 700) derived from buffalo weed (*Ambrosia trifida* L. var. *trifida*) at different pyrolysis temperatures of 300, 500 and 700°C were investigated for the removal of Cd(II) and Pb(II) ions from aqueous solutions. The physicochemical properties of the biochars were studied using FTIR, scanning electron microscopy (SEM), X-ray diffraction, Brunauer, Emmett and Teller surface area, cation exchange capacity and energy dispersive X-ray analysis. The adsorption at solution pH=5 could be well described by Freundlich model for Cd(II) and Pb(II) in their single and mixed system with  $R^2 \geq 0.95$ . The maximum adsorption capacities of the biochar BWBC 700 from the Langmuir equation were found to be 11.63 and 333.33 mg g<sup>-1</sup> for Cd(II) and Pb(II), respectively. Pseudo-second-order kinetic model was fitted well in describing the adsorption kinetics of Cd(II) and Pb(II) onto the biochar BWBC 700. About 0.02 mol L<sup>-1</sup> disodium salt of EDTA was able to desorb Cd(II) and Pb(II) from the biochar BWBC 700 with an approximately 63.5% and 96.8% desorption yield, respectively. Ion exchange and surface complexation found to be the main mechanisms involved in the adsorption process. The developed biochar derived from *Ambrosia trifida* L. var. *trifida* found to be a low cost adsorbent and could be used for the effective removal of Cd(II) and Pb(II) in waste waters.

*Keywords:* Biochar; *Ambrosia trifida* L. var. *trifida*; Pyrolysis; Adsorption; Cadmium; Lead

### 1. Introduction

The excessive amount of toxic metals poses a global challenge to the environmental scientists and engineers. Toxic metals such as Cd(II) and Pb(II) are discharged into the environment from agricultural or industrial production, or accidental or by deliberate misuse of human actions. Cd(II) which was known to be extremely toxic [1–3], accumulates in humans, mainly in the kidneys for a relatively long time and

can also replace Zn(II) ions in some metallo-enzymes, thereby affecting the enzyme activity [4]. The higher concentrations of Pb(II) in the ecosystem have a substantial impact on the environment and Pb(II) poisoning causes various severe health problems [5–7]. Therefore, removal of these toxic metals from wastewaters prior to discharge into water and soil bodies is necessary in terms of environment and economic consideration.

There are several analytical and preconcentration methods that are employed for the quantification of

\*Corresponding author.

Cd(II) and Pb(II) ions in ultra-trace amounts from different environmental samples, however, these methods require multi-step sample manipulations, which are cost and time consuming [8–11].

At present, there is a growing interest in developing low-cost and eco-friendly adsorbents for the removal of heavy metals from the environmental samples. In this regard, different biosorbent materials have been investigated for the removal of heavy metals including Cd(II) and Pb(II) [12–16].

Biochars, a non-liquefied carbon enriched solid porous material produced from the varieties of biomass are increasing ever attention as an adsorbent for the removal of toxic pollutants from the environment and they have also been extensively studied for their application as a soil amendment [17]. The production of biochar is by pyrolysis, which is a carbonization process in which the content of carbon increases with temperature accompanied by a simultaneous decrease in oxygen and hydrogen contents [18].

Recently different biochars were developed as an adsorbents for the removal of toxic metal ions Cd(II) and Pb(II) from different environmental samples [19–24]. Mohan group investigated the biochar produced from fast pyrolysis of wood and bark during bio-oil production for the sorption of Cd(II) along with other heavy metal ions [19]. The immobilization of heavy metal ions including Cd(II) in water and soil was studied using broiler litter-derived biochars by Uchi-miya et al. [20], and the immobilization and retention of soluble Cd(II) using hardwood biochars was investigated by Beesley and Marmiroli group [21]. Pb(II) sorption capacity and mechanisms by sludge-derived biochar were investigated by Lu et al. [22]. Dairy-Manure derived biochar was effectively used for the sorption of Pb(II) by Cao group [23]. The feasibility of biochars resulted from Pine wood and Rice husk hydrothermal conversion process was investigated by Liu and Zhang for the removal of Pb(II) from water [24]. However, we find very limited literature on adsorption of Cd(II) and Pb(II) in their mixed systems using biochars. The pyrolysis conditions for biochar production, together with feedstock characteristics largely control the physical and chemical properties (e.g. composition, particle, surface area and pore size distribution) of the resulting biochar, which determine the suitability for a given application [25]. Biomass materials generally contain a considerable amount of inorganic matter, particularly alkali and alkaline earth metals, which undergoes complex transformations along with evolution of morphological and crystalline structure in biochar during the pyrolysis [26].

The ministry of Environment in South Korea basing on the Natural Environment Conservation Act,

designated six alien plant species as harmful on the ecosystem, in which buffalo weed (*Ambrosia trifida* L. var. *trifida*) was one of those species. Plant wastes are more preferred for use as a low-cost adsorbents as they are highly abundant and have various functional groups that can bind heavy metal ions such as hydroxyl, amino, carboxyl, phosphate, sulfonate and ether [27]. The previous plant waste studies indicated that physical, chemical, precipitation and ion exchange kinds of adsorption mechanisms were involved in the removal of heavy metal ions [28,29].

In the present investigation, biochars were derived from buffalo weed (*Ambrosia trifida* L. var. *trifida*), a waste plant biomass at different pyrolysis temperatures of 300, 500 and 700°C and they were assessed for the adsorption of Cd(II) and Pb(II) ions from aqueous solutions. The physicochemical properties of the developed biochars were studied using different characterization techniques such as FTIR, scanning electron microscopy (SEM), X-ray diffraction (XRD), Brunauer, Emmett and Teller (BET) surface area and cation exchange capacity (CEC). Optimum experimental conditions for adsorption of toxic metal ions Cd(II) and Pb(II) was studied. This study was evaluated for the adsorption of Cd(II) and Pb(II) ions in single and mixed system. The developed biochar found to be a low-cost, eco-friendly and potential adsorbent for the removal of toxic metal ions Cd(II) and Pb(II) from aqueous solutions.

## 2. Experimental methods

All chemical reagents used were of analytical grade. Stock Cd(II) and Pb(II) solutions ( $1,000 \text{ mg L}^{-1}$ ) were prepared by dissolving  $\text{Cd}(\text{NO}_3)_2$  (Junsei, Japan) and  $\text{Pb}(\text{NO}_3)_2$  (Samchun, Korea) in distilled water, respectively. All the pH buffer solutions used in this study were purchased from Samchun Chemicals, Korea. The adsorbate solution pH=5 was maintained using potassium hydrogen phthalate buffer.

### 2.1. Biochar preparation

The collected buffalo weed (*Ambrosia trifida* L. var. *trifida*) plants were washed repeatedly with water to remove dust and soluble impurities, dried and cut to a very fine pieces before the pyrolysis. These dried pieces of buffalo weed biomass was placed in a ceramic pot with pressed state, covered with a fitting lid and this system was flushed with dry nitrogen for 30 min to remove all traces of oxygen. Thus, the biochars were produced via pyrolyzing biomass at different temperatures for 4 h with a heating rate of  $10^\circ\text{C min}^{-1}$

using heating furnace (Thermolyne 48000, USA) in the absence of oxygen, which allows the material to be charred rather than combusted. The biochars obtained at different pyrolysis temperature of 300, 500 and 700°C were allowed to cool at room temperature under a flow of N<sub>2</sub> gas and crushed to a fine powder using batch mill (IKA A 11 basic analytical mill, Japan). The biochar yield was calculated as the ratio of the weight of the obtained dry biochar after pyrolysis to that of original dry biomass. The obtained biochar was treated by washing with dichloromethane (1:5 w/v) followed by deionized water, dried in oven at 105°C for 24 h and sieved to size 500 µm. However, 2% in weight loss of biochar was found after washing. The dried biochars were stored in air-tight plastic containers and referred as BWBC 300, BWBC 500 and BWBC 700, respectively. All the resulted biochars were subjected to structural characterization.

The biochar samples were continuously stirred for an about 1 h in distilled water (1:5 w/w) and there pH was measured using pH meter (Orion, model 720A, USA). The CEC of the biochars was studied using ammonium acetate method [30].

## 2.2. FT-IR analysis

FTIR spectrometer (Bruker Optik GMBH, IFS-66/S, Germany) equipped with a diamond crystal attenuated total reflection unit was used. The sample discs were prepared by mixing oven-dried (at 105°C) biochars with spectroscopy-grade KBr in an agate mortar. A spectrum was obtained in two replicates with 64 scans for each sample at 4 cm<sup>-1</sup> resolution from 400 to 4,000 cm<sup>-1</sup>.

## 2.3. SEM analysis

The surface morphology of the biochars obtained at different pyrolysis temperature was studied using SEM system [SEC, Nano eye SNE-1500M, South Korea].

## 2.4. XRD analysis

All the obtained biochars were subjected to the analysis of XRD to investigate the impact of the pyrolysis temperature using X-ray diffractometer (Bruker AXS, model D8 discover with GADDS, Germany) equipped with a Cu Kα<sub>1</sub> radiation source at 40 kV voltage, 40 mA current was used for the XRD analysis.

## 2.5. BET-surface area analysis

Surface area and pore characterization system (Micromeritics, ASAP 2010 model, USA) was used

for the BET surface area and pore size analysis. The pore volume and pore diameter of all the biochars along with their surface area was measured. The samples were analysed for multipoint BET surface area using low-temperature nitrogen and all the measurements were performed in triplicates.

## 2.6. Energy dispersive X-ray analysis

An amount of 1 g L<sup>-1</sup> of biochar BWBC 700 was loaded with 50 mg L<sup>-1</sup> of Cd(II) and Pb(II) in mixed system at pH 5 for a contact time of 4 h. In similar conditions, same amount of biochar without metal loaded was used as a blank, which had undergone of possible leaching of exchangeable cations into the solution during the contact time of 4 h. The EDX patterns for the blank (unloaded) and loaded biochar BWBC 700 was analysed by Energy Dispersive X-ray (EDX) system (Hitachi, model S-2500 C, Japan, accelerating voltage 0.5 kV–30 kV, resolution 149 eV).

## 2.7. Cd(II) and Pb(II) adsorption and desorption studies

A batch equilibration method was used to determine Cd(II) and Pb(II) in aqueous solutions. Adsorption experiments were conducted by varying contact time, pH, adsorbent dose and adsorbate concentration. Experiments were carried out in 50 mL polypropylene conical tubes (30 × 115 mm) by mixing 0.025 g (0.5 g L<sup>-1</sup>) of biochar with 50 mL at pH 5 solution with 0.01 mol L<sup>-1</sup> NaNO<sub>3</sub> as the background solution containing concentrations 1–50 mg L<sup>-1</sup> of Cd(II) or Pb(II) and Cd(II)+Pb(II) in single and mixed system, respectively. The metal precipitation was not observed for a period of 24 h during the experiments carried for the Cd(II) or Pb(II) concentrations in solution without biochar. The contact time and other optimum conditions were selected based on preliminary experiments, that equilibrium was established in 4 h, no further uptake occurred between 8 and 12 h. Thus, all equilibrium tests were conducted for 4 h. After this period solid and liquid phases were separated by centrifugation and the solution was filtered using 0.45 µm syringe filter for further chemical analysis. The amount of Cd(II) and Pb(II) was determined by measuring concentrations difference in before and after adsorption experiments using ICP-OES (Optima 2000 DV, Perkin Elmer, USA). The amount of Cd(II) or Pb(II) adsorbed,  $q$  (mg g<sup>-1</sup>) was calculated using the following equation:

$$q = \frac{C_0 - C_e}{m} \times V \quad (1)$$

where  $C_0$  ( $\text{mg L}^{-1}$ ) and  $C_e$  ( $\text{mg L}^{-1}$ ) are concentrations of Cd(II) or Pb(II) before and after adsorption respectively,  $m$  (g) is the weight of the biochar used and  $V$  (L) is the final volume of the aqueous solution containing Cd(II) or Pb(II). The percentage uptake of the biochar or removal percentage of Cd(II) or Pb(II) was calculated by the following equation:

$$\text{Removal \%} = \frac{C_0 - C_e}{C_0} \times 100 \quad (2)$$

One of the developed biochar (BWBC 700) was chosen for the effect of pH on the percentage removal of metal ions Cd(II) and Pb(II). In this study, a known amount of metal ions  $1 \text{ mg L}^{-1}$  or  $10 \text{ mg L}^{-1}$  concentrations of Cd(II) and Pb(II) were spiked over a pH solutions ranging from pH 2 to 6 with a final volume of 50 mL. To this  $0.05 \text{ g}$  ( $1 \text{ g L}^{-1}$ ) biochar dosage was added and equilibrated for 4 h in stirring condition. Biochar samples were separated after centrifugation and the filtrate was analysed for further chemical analysis. The percentage uptake of the biochar or removal percentage of Cd(II) or Pb(II) was calculated by the Eq. (2).

The adsorption isotherms play an important role in the predictive modeling procedures for analysis and design of adsorption systems. The Langmuir and Freundlich isotherms, which assumes a monolayer adsorption on a homogenous surface and a multilayer adsorption on a heterogeneous surface respectively, are the most frequently used models to represent the data of adsorption from the solution [31].

To estimate the removal efficiency of metal ions Cd(II) and Pb(II) in single and mixed system, Langmuir and Freundlich models were employed to evaluate the adsorption properties and for the potential application of developed biochar BWBC 700. The two linear models are as follows:

$$\frac{C_e}{q} = \frac{1}{ab} + \frac{C_e}{b} \quad [\text{Langmuir model}] \quad (3)$$

$$\log q = \log K + \frac{1}{n} \log C_e \quad [\text{Freundlich model}] \quad (4)$$

where  $C_e$  ( $\text{mg L}^{-1}$ ) is the equilibrium concentration in the solution,  $q$  ( $\text{mg g}^{-1}$ ) is the Cd(II) or Pb(II) adsorbed at equilibrium and is calculated from the Eq. (1),  $b$  ( $\text{mg g}^{-1}$ ) is the maximum adsorption capacity,  $n$  is the Freundlich constant related to adsorption intensity, and  $a$  ( $\text{L mg}^{-1}$ ) and  $K$  ( $(\text{mg g}^{-1})(\text{L mg}^{-1})^{1/n}$ ) are the adsorption constants for Langmuir and Freundlich models, respectively.

For kinetics, a biochar (BWBC 700) dosage of  $0.05 \text{ g}$  ( $1 \text{ g L}^{-1}$ ) sample was equilibrated under stirring condition in a solution having  $10 \text{ mg L}^{-1}$  of Cd(II) or Pb(II) concentrations at solution pH 5. In the similar way, different equilibration sets with same optimization conditions were prepared and for every 5 min the obtained filtrate from each successive set were analysed using ICP-OES and this was continued till a constant percentage removal was obtained. The studied adsorption kinetic data of Cd(II) and Pb(II) on the adsorbent were analysed in terms of pseudo-first-order and pseudo-second-order sorption equations. The pseudo-first-order equation was given as:

$$\log(q_e - q_t) = \log q_e - K_1 t \quad (5)$$

where  $q_e$  ( $\text{mg g}^{-1}$ ) and  $q_t$  ( $\text{mg g}^{-1}$ ) are the adsorption capacities at equilibrium and at time  $t$  (min), respectively;  $K_1$  is the first-order rate constant ( $\text{min}^{-1}$ ).

The pseudo-second-order equation was expressed as:

$$\frac{t}{q_t} = \frac{1}{K_2 q_e^2} + \frac{t}{q_e} \quad (6)$$

where  $K_2$  is the second-order rate constant ( $\text{g mg}^{-1} \text{ min}^{-1}$ ). Additionally, the initial adsorption rate,  $h$  ( $\text{mg g}^{-1} \text{ min}^{-1}$ ) can be determined from  $K_2$  and  $q_e$  values using  $h = K_2 q_e^2$ .

In the desorption studies, the biochar BWBC 700 was loaded with  $50 \text{ mg L}^{-1}$  of Cd(II) and Pb(II) in mixed system, following the general adsorption procedure described above. After adsorption, loaded biochar was dried at  $60^\circ\text{C}$  for 24 h and placed in contact with 50 mL of different desorbing solutions of either  $0.02 \text{ mol L}^{-1}$  disodium salt of EDTA or  $0.2 \text{ mol L}^{-1}$   $\text{HNO}_3$  or  $0.2 \text{ mol L}^{-1}$  HCl for 1 h under ultra sonication. The metal loaded biochar suspension was filtered and the supernatant was analysed for Cd(II) and Pb(II) ions desorbed using ICP-OES. Thereafter, desorbed efficiency of Pb(II) or Cd(II) was calculated as follows

$$\text{Desorption efficiency \%} = \frac{\text{Metal released (mg)}}{\text{Initially metal adsorbed (mg)}} \times 100 \quad (7)$$

### 3. Results and discussion

#### 3.1. Chemical and physical characterization of developed biochars

The FTIR spectra of the resulted biochars (BWBC 300, BWBC 500 and BWBC 700) pyrolysis at 300, 500

and 700°C are shown in Fig. 1. Here the distinguishable bands observed between wave numbers 4,000–400  $\text{cm}^{-1}$  shows that the spectrum of the biochars was different in shape and intensity, indicating that different thermal decomposition process has undergone during the pyrolysis. The results indicate that the developed biochars mainly consists of aromatic functional groups. The peaks between 700–900  $\text{cm}^{-1}$  was assigned to an aromatic C–H stretching. The peak at 1,019 and 1,034  $\text{cm}^{-1}$  corresponds to ether C–O and alcohol C–O stretching. The peaks between 1,409 and 2,588  $\text{cm}^{-1}$  corresponds to aromatic C=C ring stretching. The peaks at 2,933 and 3,023  $\text{cm}^{-1}$  corresponds to C–H stretching vibration and the peak at 3,308  $\text{cm}^{-1}$  corresponds to OH stretching and this may be due to acid or alcohol structures. From Fig. 1, it can also be seen that the major peaks are present in the biochars developed at 300 and 500°C temperatures, whereas

they are absent in the biochar produced at 700°C, showing a quite flat spectrum, indicating that all phenols and ether groups have been decomposed. However, the biochars obtained at various temperatures found to have structural difference and this may be due to the difference in the cell wall composition of the biochars and these can be clearly seen from the surface morphological studies shown in Fig. 2 using SEM. The biochar samples BWBC 300 and BWBC 500 which was known to be rich in carbon contains more holes than BWBC 700, because of evaluation of volatile matter during the pyrolysis. As the average particle sizes become smaller at higher temperature 700°C, the biochar sample BWBC 700 has different structure which could result in the higher surface area of biochar when compared to other biochars.

The XRD patterns of the developed biochars are given in Fig. 3. In all the biochars, the absence of

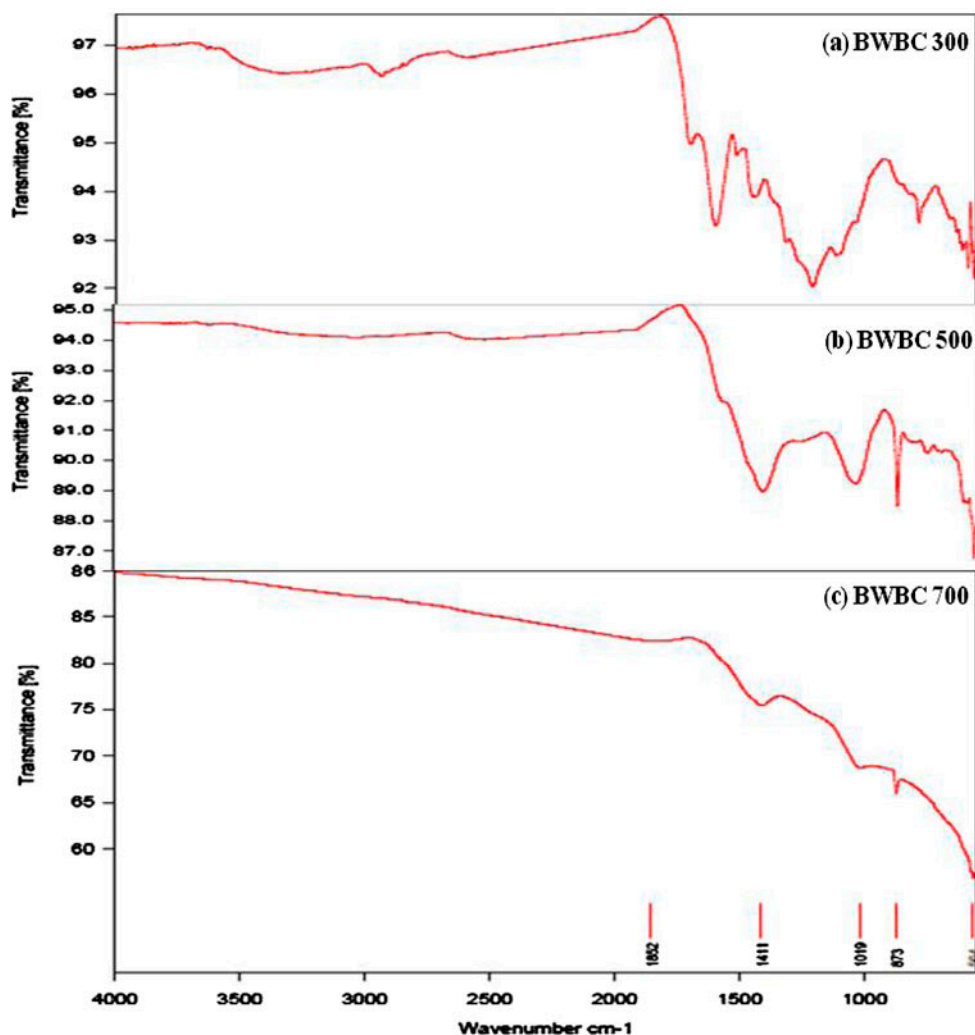


Fig. 1. FTIR Spectrum of buffalo weed (*Ambrosia trifida* L. var. *trifida*) biochars pyrolysis at temperatures (a) 300°C, (b) 500°C and (c) 700°C.

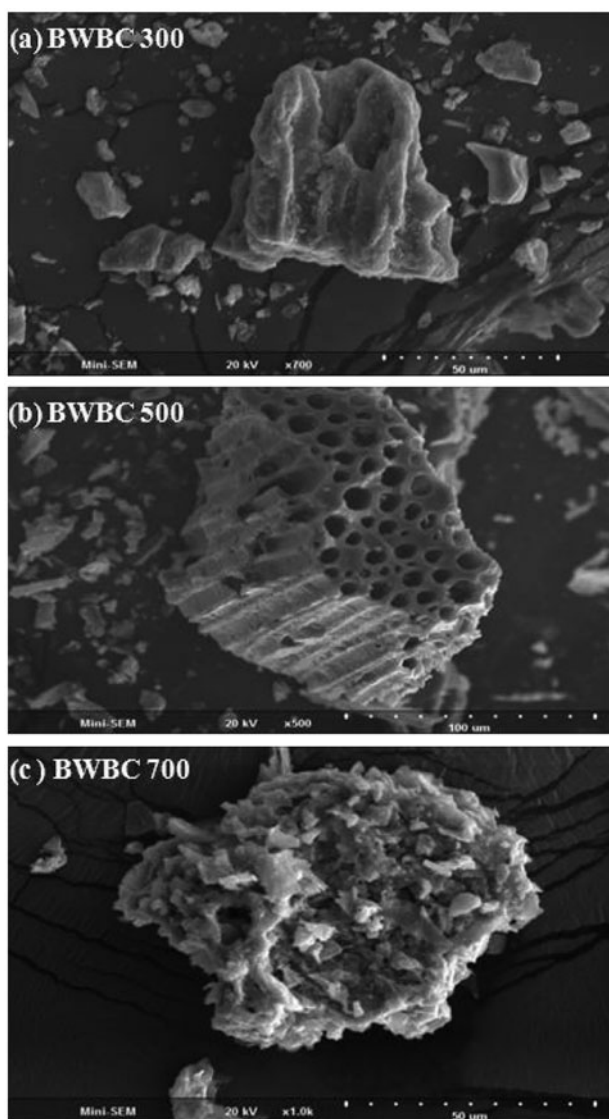


Fig. 2. SEM images of buffalo weed (*Ambrosia trifida* L. var. *trifida*) biochars pyrolysis at temperatures (a) 300°C, (b) 500°C and (c) 700°C.

peaks in between  $2\theta=15.3^\circ$  and  $2\theta=22.4^\circ$  are assigned to the absence of crystallographic planes of the crystalline regions of cellulose or decrease of crystallographic planes of the crystalline regions of cellulose. In biochars BWBC 500 and BWBC 700 the peak at  $2\theta=24.7^\circ$  is the low pattern in cellulose crystallinity. The peaks around  $2\theta=42.7^\circ$  to  $2\theta=44.8^\circ$  indicates the formation of turbostratic carbon crystallites [32]. The presented results of XRD patterns are a further indication of the structural differences between chars consisting of turbostratic carbon crystallites (Fig. 2).

The BET method was used to determine the total surface area of all developed biochars. The physical

structure properties of the biochars are summarized in Table 1. In all the developed biochars, as the pyrolysis temperature increases, the BET surface area increased, this may be due to high temperature and long residence time of the reaction conditions, the porous structure of biochar was cracked and the pores were partially blocked as a result of the repolymerization/recondensation of water soluble compounds [33]. This could have resulted in the lesser increase in surface area of biochars at higher temperature. It was also found that as the pyrolysis temperature increases, the maximum pore volume also increased. This is due to that under some conditions, a high temperature causes micropores to widen because it may destroy the walls between adjacent pores, resulting in the enlargement of pores. This leads to a decrease in the fraction of volume found in the micropore range and an increase in the total pore volume. As seen from Table 1, all the obtained biochars has pore diameter in the order  $20 < d < 500 \text{ \AA}$ , which can be classified as mesopores [34].

The ammonium acetate method was used to study the CEC of biochars. The exchangeable cations such as Ca, K, Na and Mg present on the negative sites of the biochar were measured using ICP-OES and the results were shown in Table 2. From the same Table 2, it also can be seen that the biochar yield decreased from 50.1 to 31.4% with increase of pyrolysis temperature. This is due to the significant loss of volatile matter, dehydration of hydroxyl groups and the degradation of cellulose structure [32]. This was supported by FTIR spectra and the XRD patterns. As a result, the pH of both buffalo weed biomass and biochars developed increased from 6.9 to 13.3 with the increase in pyrolysis temperature. The differences in structural changes as a function of temperature have also important consequences in terms of charge characteristics of the biochar produced under different conditions. These changes in turn are responsible for their CEC, which proved to be very low at low-temperatures and increases significantly at higher temperatures [34]. Thus, biochar BWBC 700 produced at higher temperature found to have more CEC of  $1,209 \text{ cmol kg}^{-1}$  than other developed biochars. Hence, pH effect on the adsorption of metal ions Cd(II) and Pb(II) was studied using the biochar BWBC 700 and this was shown in Fig. 4.

### 3.2. Effect of pH

From Fig. 4, it was observed that the percentage removal of metal ions Cd(II) or Pb(II) increased with increasing adsorbate solution pH and a maximum value was reached at an equilibrium pH of around 5 and 6 for Pb(II) and Cd(II), respectively. It was reported that formation of Pb(II) and Cd(II) hydrolysis

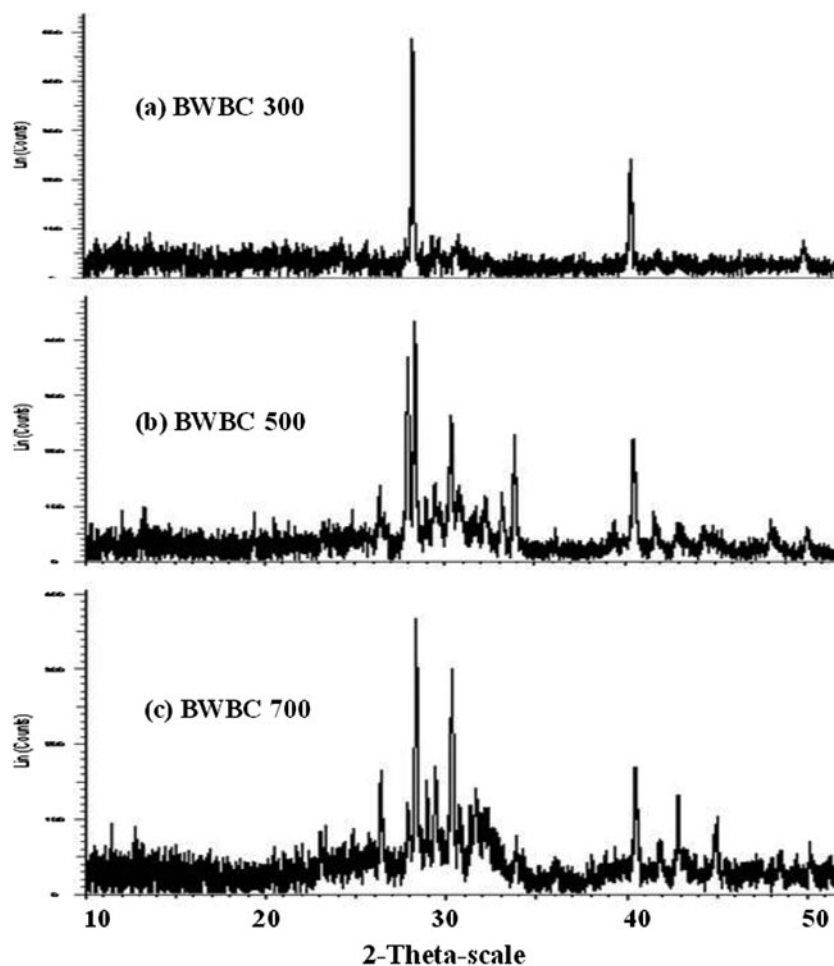


Fig. 3. X-ray diffraction patterns of buffalo weed (*Ambrosia trifida* L. var. *trifida*) biochars pyrolysis at temperatures (a) 300°C, (b) 500°C and (c) 700°C.

products occur at  $\text{pH} > 6$  [12,19]. Hence, the studies beyond  $\text{pH} = 6$  were not attempted. The decrease in percentage removal of metal ions at lower  $\text{pH}$  was

Table 1

Surface structure properties of buffalo weed (*Ambrosia trifida* L. var. *trifida*) biochars derived at pyrolysis temperatures 300°C, 500°C and 700°C

Parameters	BWBC 300	BWBC 500	BWBC 700
BET surface area ( $\text{m}^2 \text{g}^{-1}$ )	1.35	4.83	279.8
Langmuir surface area ( $\text{m}^2 \text{g}^{-1}$ )	1.77	6.61	334.9
Micropore area ( $\text{m}^2 \text{g}^{-1}$ )	0.36	0.44	209.4
External surface area ( $\text{m}^2 \text{g}^{-1}$ )	0.99	4.39	70.4
Micropore volume (v/v %)	2.40	3.80	53.0
Average pore diameter (Å)	152.7	194.4	22.4
Maximum pore volume ( $\text{cm}^3 \text{g}^{-1}$ )	0.0051	0.023	0.1567

due to the competition of hydrogen ions with the existing metal ions in the solution. While increasing solution  $\text{pH}$ , the coordinate of available cations with  $\text{Cd(II)}$  and  $\text{Pb(II)}$  resulted in higher removal rate. Further, experiments were performed at an adsorbate solution  $\text{pH} 5$  for  $\text{Cd(II)}$  and  $\text{Pb(II)}$  in order to correlate metal removal with the adsorption process in their mixed system.

### 3.3. Metal removal efficiency of developed biochars

The biochars developed at various pyrolysis temperatures (300, 500 and 700°C) were investigated for the removal efficiency of the metal ions  $\text{Cd(II)}$  and  $\text{Pb(II)}$  which was shown in Fig. 5. Here the batch experiment for a contact time of 4 h was carried out by stirring 0.05 g ( $1 \text{ g L}^{-1}$ ) of biochar with 50 mL solution at  $\text{pH} 5$  containing  $10 \text{ mg L}^{-1}$  of  $\text{Cd(II)}$  or  $\text{Pb(II)}$ . It was observed that the biochar developed at 700°C (BWBC 700) found to have >98% removal capacity of

Table 2

CEC, pH and yield of buffalo weed (*Ambrosia trifida* L. var. *trifida*) biochars derived at pyrolysis temperatures 300°C, 500°C and 700°C

Adsorbent	pH	CEC (cmol kg <sup>-1</sup> )	Exchangeable base cations (cmol kg <sup>-1</sup> )				Yield (w/w%)
			Ca	K	Na	Mg	
Raw BW	6.9	260.8	3.38	1.88	247.4	7.11	100
BWBC 300	10.9	768.7	3.11	721.6	8.59	1.35	50.1
BWBC 500	12.1	1,261.8	0.09	1,208.1	9.48	0.17	35.3
BWBC 700	13.3	1,268.7	0.34	1,209	9.33	1.06	31.4

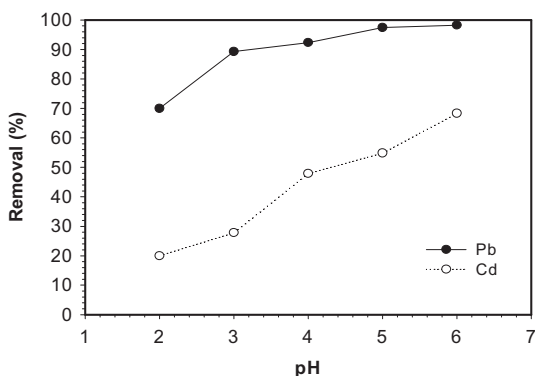


Fig. 4. Removal of Cd(II) and Pb(II) metal ions using biochar BWBC 700 as a function of pH (biochar dosage = 1 g L<sup>-1</sup>, initial Cd(II) or Pb(II) concentration = 1 mg L<sup>-1</sup>, contact time = 4 h).

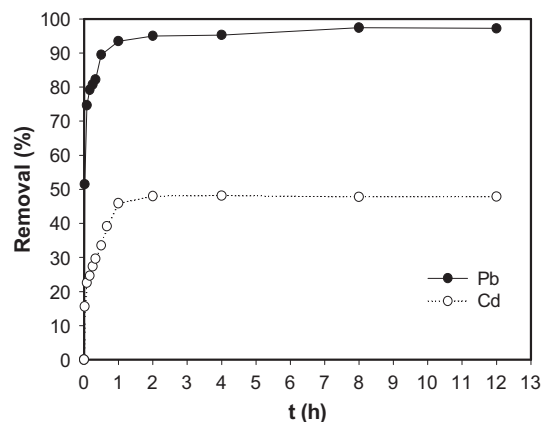


Fig. 6. Effect of contact time on the removal of Cd(II) and Pb(II) onto biochar BWBC 700 (biochar dosage = 1 g L<sup>-1</sup>, initial Cd(II) or Pb(II) concentration = 10 mg L<sup>-1</sup>, solution pH = 5).

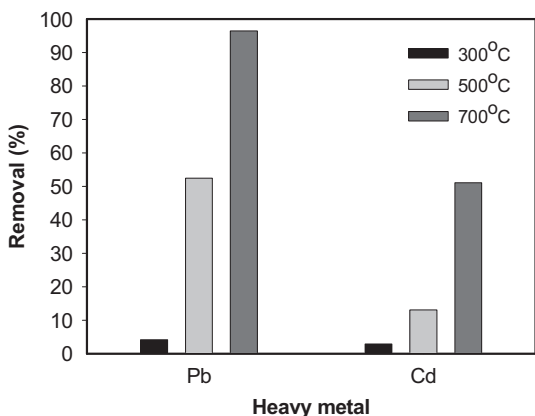


Fig. 5. Removal of Cd(II) and Pb(II) using buffalo weed (*Ambrosia trifida* L. var. *trifida*) biochars pyrolysis at temperatures 300°C, 500°C and 700°C (biochar dosage = 1 g L<sup>-1</sup>, initial Cd(II) or Pb(II) concentration = 10 mg L<sup>-1</sup>, solution pH = 5, contact time = 4 h).

metal ions Cd(II) and Pb(II). The biochars BWBC 300 and BWBC 500, due to their lower initial pH, the surface oxygen linked to H<sup>+</sup>, making them inaccessible for metal ions. As shown in Table 1, the progressive increase of surface area from BCBW 300 to BCBW 700

may be due to change in crystal structure. BWBC 700 found to have larger surface area with greater micropore volume 53%, with an average pore diameter of 22.4 Å, indicates that this biochar was rich in mesopores, whose walls are formed by a large number of adsorbent atoms or molecules, which means that the adsorbent has also the possibility of surface complexation. As shown in Table 2, CEC values greatly increased above 300°C. The all other remaining experiments were carried out using the biochar BWBC 700 as the order of removal capacity of metal ions Cd(II) and Pb(II) found to be BWBC 700 > BWBC 500 > BWBC 300. The higher removal capacity of Cd(II) and Pb(II) by biochar BWBC 700 can be attributed to the increase number of available sites for surface complexation and also availability of exchangeable cations for the adsorption.

#### 3.4. Effect of contact time

The profile of contact time of Cd(II) and Pb(II) ions removal in the BWBC 700 sample from 50 mL aqueous solution at pH 5 was shown in Fig. 6. From Fig. 6, the



equilibration time required for the saturation loading of Cd(II) or Pb(II) in the biochar was found to be about 4 h and no further removal occurred between 8 h and 12 h.

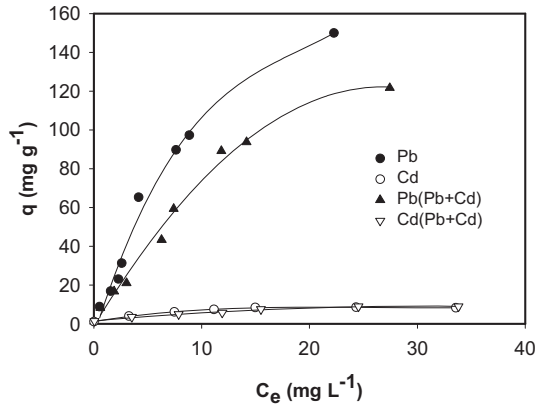


Fig. 7. Adsorption isotherms of Cd(II) and Pb(II) metal ions in single and mixed systems by biochar BWBC 700 (biochar dosage =  $0.5 \text{ g L}^{-1}$ , initial Cd(II) or Pb(II) concentration =  $1\text{--}50 \text{ mg L}^{-1}$ , solution pH = 5, contact time = 4 h).

### 3.5. Adsorption isotherms

Fig. 7 shows the experimental adsorption isotherms, that the amount of Cd(II) or Pb(II) or both metal ions adsorbed at the equilibrium at solution pH 5 with a biochar dosage of  $0.025 \text{ g}$  ( $0.5 \text{ g L}^{-1}$ ) and metal ion concentrations ranging from  $1$  to  $50 \text{ mg L}^{-1}$ , where  $C_e$  ( $\text{mg L}^{-1}$ ) was the final equilibrium concentration of metal remaining in the solution and  $q$  ( $\text{mg g}^{-1}$ ) was the amount of metal uptake. To gain some insight into the adsorption process between Cd(II) or Pb(II) in single and mixed systems onto the biochar BWBC 700, the equilibrium adsorption data of Cd(II), Pb(II), Cd(II) in Cd(II)+Pb(II) mixture and Pb(II) in Cd(II)+Pb(II) mixture were fitted into the linear forms of Langmuir (Fig. 8) and Freundlich (Fig. 9) isotherms. The relative parameters calculated from the two models using the Eqs. (3) and (4) were listed in Table 3. The Langmuir isotherm parameter  $b$  ( $\text{mg g}^{-1}$ ) indicated the maximum adsorption capacity of the adsorbent and the value calculated from Langmuir equation was found to be  $11.63 \text{ mg g}^{-1}$  and  $333 \text{ mg g}^{-1}$  for Cd(II) and Pb(II), respectively. The higher value of “ $b$ ” for Pb(II) than for Cd(II)

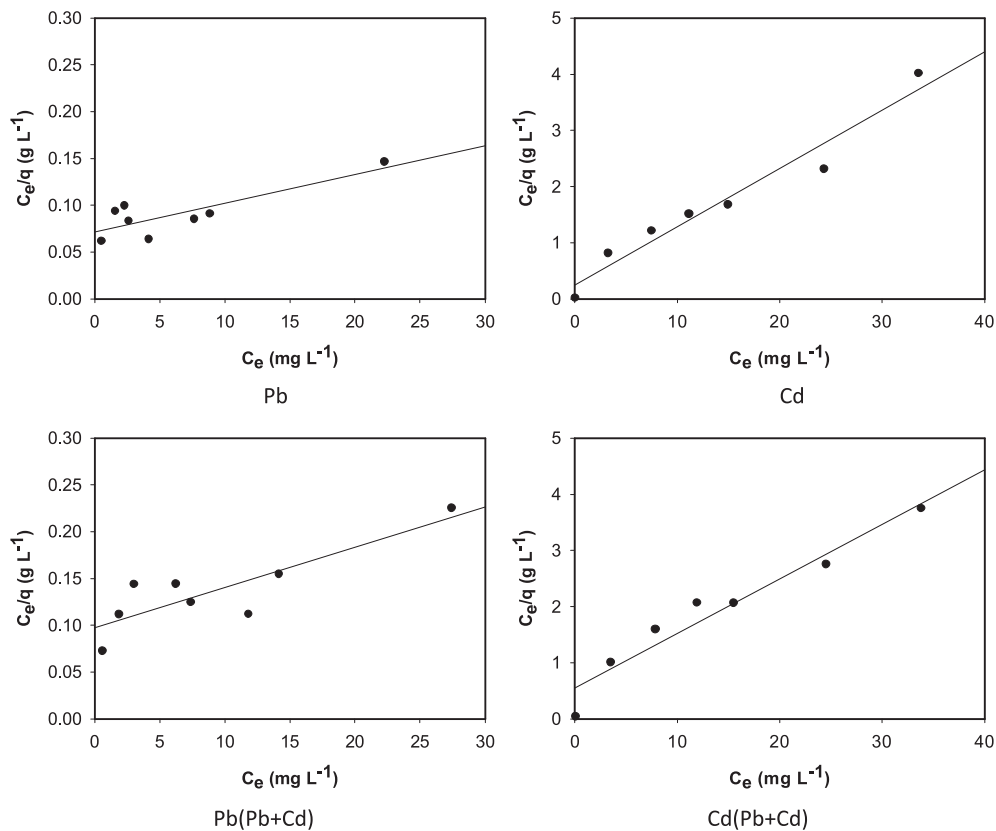


Fig. 8. Langmuir isotherm model for Cd(II) and Pb(II) adsorption onto the biochar BCBW 700 in single and in mixed system.

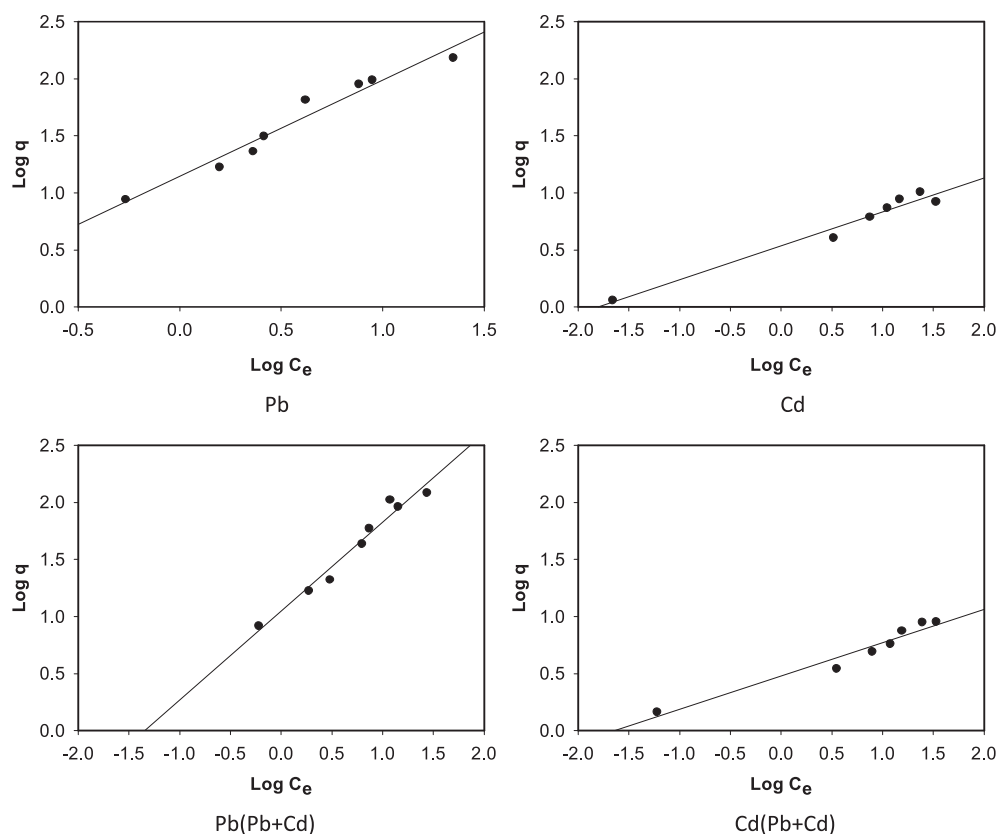


Fig. 9. Freundlich isotherm model for Cd(II) and Pb(II) adsorption onto the biochar BCBW 700 in single and in mixed system.

Table 3  
Isotherm constants for adsorption of Cd(II) and Pb(II) onto biochar BWBC 700 in single and in mixed system

Adsorbed metal	Langmuir isotherm			Freundlich isotherm		
	<i>a</i>	<i>b</i> (mg g <sup>-1</sup> )	<i>R</i> <sup>2</sup>	1/ <i>n</i>	<i>k</i>	<i>R</i> <sup>2</sup>
Pb(II)	0.04	333.33	0.688	0.840	14.00	0.959
Cd(II)	0.22	11.63	0.962	0.307	3.48	0.975
Pb(II)-Pb(II)+Cd(II)	0.04	250.00	0.795	0.769	11.12	0.977
Cd(II)-Pb(II)+Cd(II)	0.18	10.31	0.938	0.292	3.01	0.954

indicates that more moles of lead ions can be adsorbed on the BWBC 700 at the equilibrium. When a solution of the mixed metals were studied, a reduction in the Cd(II) adsorption was observed showing a clear competition between the metals probably due to a lower attraction of this metal towards the corresponding active sites of the biochar, this could be due to differences in the hydration of Pb(II) and Cd(II) ions. Since the radius of Cd(II) (0.92 Å) is considerably smaller than that of Pb(II) (1.33 Å), Cd(II) ions are easier to hydrate than Pb(II),

thereby forming a thicker water layer on the surface. Consequently, Cd(II) is more mobile in solution and would have a lesser tendency to adsorb on the biochar [35]. However, the obtained results shows that the adsorption at solution pH 5 could be well described by Freundlich model, as it presents greater correlation coefficient for Cd(II) and Pb(II) in single and mixed system with  $R^2 > 0.95$ . As the Freundlich model was characterized by  $1/n$ , the heterogeneity factor, the values of  $1/n$  obtained in the present work are between  $0.1 < 1/n < 1.0$  which represents good adsorption of metal ions. The similar behavior of Cd(II) and Pb(II) adsorption process fitting to Freundlich isotherm with exclusively involvement of ion exchange, physical sorption and chelation mechanism was reported by Pehlivan et al. and Li et al. [13,31]. The fact that the Freundlich isotherm fits the data in the present work may be due to heterogeneous distribution of active sites and the supply of these adsorption sites was infinite on studied biochar surface. The fitting of the Freundlich isotherm to the experimental data for biochar BWBC 700 can be explained by the fact that this model can only be applied in the low to intermediate concentration

range. The Langmuir isotherm failed to apply in this instance could indicate that the adsorption of Cd(II) and Pb(II) ions does not assume monolayer mechanism [19]. Thus, the adsorption of biochar BWBC 700 involves coverage of multi molecular layers, as the most actively energetic sites are occupied first and thereafter the surface was occupied until the lowest energy sites were filled at the final stage of the adsorption process. In addition, physical adsorption may also be responsible for the interaction between adsorbent and metal ions because biochar BWBC 700 had a large surface area.

### 3.6. Adsorption kinetics

In the present investigation, the two kinetic models, pseudo-first-order and pseudo-second-order were used to fit the experimental data using the Eqs. (5) and (6), respectively. The obtained kinetic parameters of the adsorption calculated from the linear plots of  $\log(q_e - q_t)$  vs.  $t$  and  $t \cdot q_t^{-1}$  of pseudo-first-order and pseudo-second-order (Fig. 10) respectively, together with the corresponding correlation coefficients ( $R^2$ ) are summarized in Table 4. The correlation coefficients  $R^2 = 0.979$  and  $R^2 = 0.999$  for the pseudo-second-order model are higher in comparison with the  $R^2 = 0.904$  and  $R^2 = 0.914$  with the pseudo-first-order kinetic

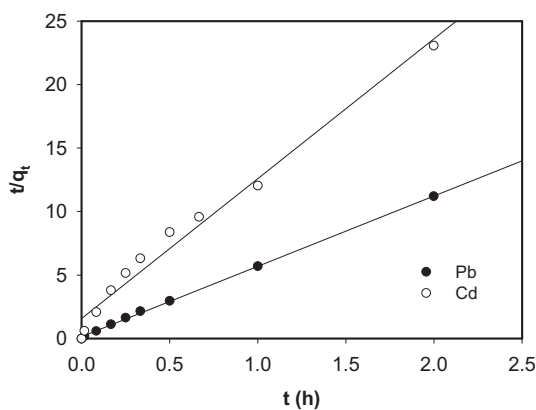


Fig. 10. Pseudo-second-order kinetics for Cd(II) and Pb(II) adsorption onto the biochar BCBW 700.

model for Cd(II) and Pb(II), respectively. This indicates that the pseudo-second-order kinetic model was fitted well in describing the adsorption kinetics of Cd(II) and Pb(II) onto the biochar BCBW 700, which suggests that the process controlling the rate may be a chemical adsorption involving exchanging of cations between adsorbent and the adsorbate [36].

### 3.7. Adsorption mechanism

For the confirmation of possible ion exchange mechanism involved in adsorption process, the blank and loaded biochar BWBC 700 with Cd(II) and Pb(II) were subjected to EDX analysis. The X-ray spectrum observed was shown in Fig. 11 and the obtained cation weight ratios were summarized in Table 5. The results shows that the decrease of weight percentage of available cations on the loaded biochar was due to that heavy metals Cd(II) and Pb(II) are taken up from the solution predominantly in exchange for cations Na, Mg, K and Ca present in the biochar BWBC 700.

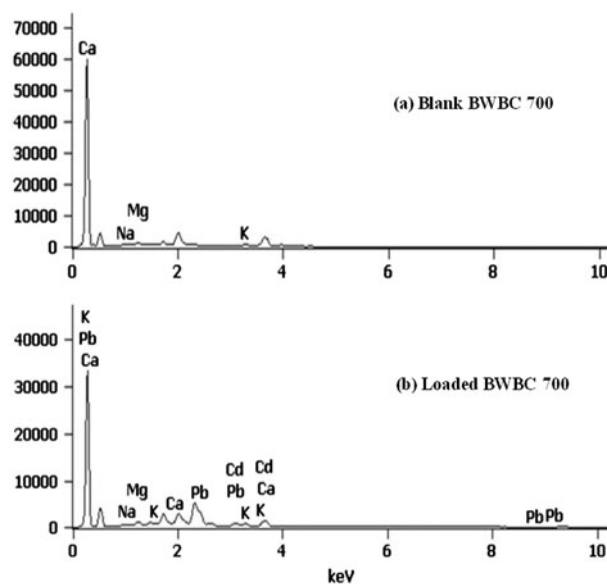


Fig. 11. EDX analysis of biochar BWBC 700 (a) blank and (b) loaded with Cd + Pb.

Table 4

Kinetic parameters for the adsorption of Cd(II) and Pb(II) onto biochar BWBC 700 based on the pseudo-first and pseudo-second-order equations

	Pseudo-first-order		Pseudo-second-order			
	$k_1$ ( $\text{min}^{-1}$ )	$R^2$	$k_2$ ( $\text{g mg}^{-1} \text{min}^{-1}$ )	$h$ ( $\text{mg g}^{-1} \text{min}^{-1}$ )	$q_e$ ( $\text{mg g}^{-1}$ )	$R^2$
Cd(II)	0.0415	0.904	0.021	0.637	5.464	0.979
Pb(II)	0.0415	0.914	0.055	6.452	10.870	0.999

Table 5  
Weight percentage of cations present in biochar BCBW 700 before and after adsorption

	Weight % of cations					
	Cd	Pb	Na	Mg	K	Ca
BWBC 700 (blank)	–	–	3.29	12.55	7.47	76.69
Loaded BCBW 700	12.40	72.68	0.72	1.34	1.38	11.48

This shows that the ion exchange mechanism was involved in the adsorption process of Cd(II) and Pb(II) onto the biochar BWBC 700. Generally, the adsorption capacity of a material depends on its surface area. Here, BWBC 700 has a high BET surface area, which results in the generation of more mesopores having the capability of primary uptake of Cd(II) and Pb(II), involving surface adsorption. However, from the EDX analysis, the higher adsorption of Pb(II) than Cd(II) on to the biochar may due to the presence of Ca and K in high amounts, as they have been shown to be actively involved in the ion exchange with Pb(II). The electronegativity values for Cd(II) and Pb(II) are 1.69 and 2.33, respectively. Again this fact would explain the higher affinity of the adsorption for Pb(II) compared to Cd(II).

Thus, in the present work the order of the adsorption capacity and kinetics was found as Pb(II) > Cd(II). This affinity order was same as in the single and mixed metal adsorption system, as the enthalpy of hydration of Cd(II) ( $-1807 \text{ kJ mol}^{-1}$ ), which is appreciably greater in magnitude than that of Pb(II) ( $-1,481 \text{ kJ mol}^{-1}$ ) which reflects a stronger interaction of Cd(II) with the coordinated water [37]. Consequently, Pb(II) ions interact more effectively with the active sites available on the biochar and with available exchangeable cations, resulting highest removal of Pb(II) than Cd(II) by the biochar BWBC 700. The obtained results are in agreement with earlier findings [38] that Pb(II) has more affinity and uptake capacity than Cd(II) on a selected adsorbent. Moreover, no significant sorption of Cd(II) was also observed by previous studies on biomass materials under various physical–chemical conditions [39]. The maximum adsorption amounts obtained in the present study were compared with the maximum metal adsorption amounts reported for other adsorbents and the developed biochar found to be more efficient than granular and powder activated carbon in removal of Cd(II) and Pb(II) [40].

### 3.8. Desorption efficiency

The desorption efficiency of biochar BWBC 700 adsorbent was studied using  $0.02 \text{ mol L}^{-1}$  disodium salt

of EDTA,  $0.2 \text{ mol L}^{-1}$   $\text{HNO}_3$  and  $0.2 \text{ mol L}^{-1}$  HCl to make the adsorption process more economical and applicable. Washing the metal adsorbed biochar with distilled water exhibited no desorption quality. It was observed that highest desorption for Cd(II) and Pb(II) to be 63.5 and 96.8%, respectively with disodium salt of EDTA. The desorbed concentration of Pb(II) was higher than that of Cd(II), which was due to higher complex formation ability of Pb(II) with EDTA due to its greater radius than Cd(II). Moreover, the stability constants ( $\log K_s$ ) of Pb(II)-EDTA and Cd(II)-EDTA complex formation are 18.8 and 16.4, respectively [41]. This could be the possible reason for the low Cd(II) removal using EDTA as a desorbing agent. However, desorption efficiency was found to be 55.0 and 10.9% for Cd(II) and 81.1 and 23.2% for Pb(II) in  $0.2 \text{ mol L}^{-1}$   $\text{HNO}_3$  and  $0.2 \text{ mol L}^{-1}$  HCl, respectively. This findings also suggest that the ion exchange was one of the main mechanism involved for the desorption process. The possible higher concentrations of acid reagents were not tried for desorption as we found deterioration effect on metal adsorption during reusability may due to physical damage of biochar. As it was also found to be difficult to collect the same amount of adsorbed biochar in each cycle, thus the desorption efficiency can be better performed in column method rather than the batch method.

### 3.9. Advantages of the method

The present study indicates that the biochar derived at high pyrolysis temperature has large surface area, increase in pore volumes and rich in mesopores. The developed biochar BWBC 700 had predominantly mesopores, which make more suitable for liquid phase adsorption for which it can be successfully applied for wastewater treatment or drinking water purification. Moreover, the proposed biochar BWBC 700 found to be low-cost and free from hazardous chemicals, when compared to activated carbon. Thus, the developed biochar can be successfully applied for the removal of Cd(II) and Pb(II) ions in their mixed system. Considering the beneficial characteristics, the developed biochar BWBC 700 can be investigated as an approach to carbon sequestration, as it is more difficult to convert back the biochar to  $\text{CO}_2$  again.

## 4. Conclusions

In the present investigation, the biochar obtained from waste plant buffalo weed (*Ambrosia trifida* L. var. *trifida*) biomass pyrolysis at  $700^\circ\text{C}$  was used to remove Cd(II) and Pb(II) from aqueous solutions. A high BET surface area biochar could be derived from (*Ambrosia trifida* L. var. *trifida*) at pyrolysis temperature  $700^\circ\text{C}$ .

The order of removal capacity of metal ions Cd(II) and Pb(II) in developed biochars found to be BWBC 700 > BWBC 500 > BWBC 300. The developed biochar allowed multilayer adsorption to take place on the surface of the adsorbent and this could be well described by Freundlich model for Cd(II) and Pb(II) in single and mixed system with  $R^2 > 0.95$  at solution pH 5. The maximum adsorption capacity from Langmuir equation was found to be 11.63 and 333 mg g<sup>-1</sup> for Cd (II) and Pb(II), respectively. In this study, pseudo-second-order kinetic model was fitted well in describing the adsorption kinetics of Cd(II) and Pb(II) onto the biochar BCBW 700. Ion exchange and surface complexation was found to be the main mechanisms involved in the present adsorption process. The present study involves free of toxic compounds and the developed adsorbent found to be more efficient than granular and powder activated carbon in removal of Cd(II) and Pb(II). The developed biochar BWBC 700 found to be rich in mesopores, which it can be successfully applied for waste water treatment or drinking water purification in large scale studies and this work is under progress. Considering buffalo weed (*Ambrosia trifida* L. var. *trifida*) as a harmful and non-usage plant in the ecosystem, the biochar obtained from this biomass turned out to be a cheap and green alternative to activated carbon for the removal of Cd(II) and Pb(II) in their mixed system.

### Acknowledgements

This investigation was supported by Korea Ministry of Environment as “The GAIA Project–2013” (sanction no: G111-17003-0038-2) and partially by a Research Grant-2012 from Kwangwoon University, Seoul, South Korea.

### References

- [1] F.A. Cotton, G. Wilkinson, C.A. Murillo, M. Bochmann, *Advanced Inorganic Chemistry*, sixth ed., Wiley, New York, NY, 1999.
- [2] The International Cadmium Association, ICdA Europe, Brussels. Available from: <http://www.cadmium.org> accessed April 10, 2006.
- [3] Agency for Toxic Substances and Disease Registry, Atlanta, Georgia. Available from: <http://www.atsdr.cdc.gov> accessed April 10, 2006.
- [4] International Agency for Research on Cancer (IARC), *Mono-graphs on the Evaluation of Carcinogenic Risks of Compounds*, vol. II, IARC, New York, NY, 1976, p. 3974.
- [5] M. Khajeh, Z.S. Heidari, E. Sanchooli, Synthesis characterization and removal of lead from water samples using lead-ion imprinted polymer, *Chem. Eng. J.* 166 (2011) 1158–1163.
- [6] D.M. Roundhill, Novel strategies for the removal of toxic metals from soils and waters, *J. Chem. Educ.* 81 (2004) 275–282.
- [7] Q.W. Yanga, W.S. Shua, J.W. Qiub, H.B. Wanga, C.Y. Lan, Lead in paddy soils and rice plants and its potential health risk around Lechang Lead/Zinc Mine, Guangdong, China, *Environ. Int.* 30 (2004) 883–889.
- [8] F. Kummrow, F.F. Silva, R. Kuno, A.L. Souza, P.V. Oliveira, Biomonitoring method for the simultaneous determination of cadmium and lead in whole blood by electrothermal atomic absorption spectrometry for assessment of environmental exposure, *Talanta* 75 (2008) 246–252.
- [9] S. Abbasi, K. Khodarahmiyan, F. Abbasi, Simultaneous determination of ultra trace amounts of lead and cadmium in food samples by adsorptive stripping voltammetry, *Food Chem.* 128 (2011) 254–257.
- [10] A.N. Anthemidis, K.I.G. Ioannou, Development of a sequential injection dispersive liquid–liquid microextraction system for electrothermal atomic absorption spectrometry by using a hydrophobic sorbent material: Determination of lead and cadmium in natural waters, *Anal. Chim. Acta* 668 (2010) 35–40.
- [11] E.M. Gama, A.S. Lima, V.A. Lemos, Preconcentration system for cadmium and lead determination in environmental samples using polyurethane foam/Me-BTANC, *Journal of Hazardous Materials, B* 136 (2006) 757–762.
- [12] R. Vimala, N. Das, Biosorption of cadmium (II) and lead (II) from aqueous solutions using mushrooms: A comparative study, *J. Hazard. Mater.* 168 (2009) 376–382.
- [13] E. Pehlivan, B.H. Yanik, G. Ahmetli, M. Pehlivan, Equilibrium isotherm studies for the uptake of cadmium and lead ions onto sugar beet pulp, *Bioresour. Technol.* 99 (2008) 3520–3527.
- [14] R. Apiratikul, V. Madacha, P. Pavasant, Kinetic and mass transfer analyses of metal biosorption by *Caulerpa lentillifera*, *Desalination* 278 (2011) 303–311.
- [15] L. Huang, Y.Y. Sun, Q.K. Yue, Q. Yue, L. Li, B. Gao, Adsorption of Cd(II) on lotus stalks-derived activated carbon: Batch and column studies, *Desalination and Water Treatment* 41 (2012) 122–130.
- [16] Y. Ma, B. Shen, R. Sun, W. Zhou, Y. Zhang, Lead(II) biosorption of an Antarctic sea-ice bacterial exopolysaccharide, *Desalin. Water Treat.* 42 (2012) 202–209.
- [17] D.A. Laird, R.C. Brown, J.E. Amonette, J. Lehmann, Review of the pyrolysis platform for coproducing bio-oil and biochar, *Biofuel. Bioprod. Bior.* 3 (2009) 547–562.
- [18] W. Zheng, M. Guo, T. Chow, D.N. Bennett, N. Rajagopalan, Sorption properties of green waste biochar for two triazine pesticides, *J. Hazard. Mater.* 181 (2010) 121–126.
- [19] D. Mohan, C.U. Pittman, Jr, M. Bricka, F. Smith, B. Yancey, J. Mohammad, P.H. Steele, M.F. Alexandre-Franco, V. Serrano, H. Gong, Sorption of arsenic, cadmium, and lead by chars produced from fast pyrolysis of wood and bark during bio-oil production, *J. Colloid Interface Sci.* 310 (2007) 57–73.
- [20] M. Uchimiya, I.M. Lima, K. Thomas Klasson, S. Chang, L.H. Wartelle, J.E. Rodgers, Immobilization of heavy metal ions (Cu(II), Cd(II), Ni(II), and Pb(II)) by Broiler Litter-derived biochars in water and soil, *J. Agric. Food Chem.* 58 (2010) 5538–5544.
- [21] L. Beesley, M. Marmiroli, The immobilisation and retention of soluble arsenic, cadmium and zinc by biochar, *Environ. Pollut.* 159 (2011) 474–480.
- [22] H. Lu, W. Zhang, Y. Yang, X. Huang, S. Wang Rongliang Qiu, Relative distribution of Pb<sup>2+</sup> sorption mechanisms by sludge-derived biochar, *Water Res.* 46 (2012) 854–862.
- [23] X. Cao, L. Ma, B. Gao, W. Harris, Dairy-manure derived biochar effectively sorbs lead and atrazine, *Environ. Sci. Technol.* 43 (2009) 3285–3291.
- [24] Z. Liu, F. Zhang, Removal of lead from water using biochars prepared from hydrothermal liquefaction of biomass, *J. Hazard. Mater.* 167 (2009) 933–939.
- [25] F. Verheijen, S. Jeffery, A.C. Bastos, M. Van der Velde, I. Diafas, Biochar application to soils: A critical scientific review of effects on soil properties processes and functions, European Commission, [http://eusoils.jrc.ec.europa.eu/esdb\\_archive/eusoils\\_docs/other/EUR24099.pdf](http://eusoils.jrc.ec.europa.eu/esdb_archive/eusoils_docs/other/EUR24099.pdf), 2010.
- [26] M. Xu, C. Sheng, Influences of the heat-treatment temperature and inorganic matter on combustion characteristics of corn-stalk biochars, *Energy Fuels* 26 (2012) 209–218.

- [27] M.A.K.M. Hanafiah, H. Zakaria, W.S. Wan Ngah, Preparation, characterization, and adsorption behavior of Cu(II) ions onto alkali-treated weed (*Imperata cylindrica*) leaf powder, *Water Air Soil Pollut.* 201 (2009) 43–53.
- [28] W.S. Wan Ngah, M.A.K.M. Hanafiah, Adsorption of copper on rubber (*Hevea brasiliensis*) leaf powder: Kinetic, equilibrium and thermodynamic studies, *Biochem. Eng. J.* 39 (2008) 521–530.
- [29] F. Veglio, F. Beolchini, Removal of metals by biosorption: A review, *Hydrometallurgy* 44 (1997) 30–316.
- [30] M. Pansu, J. Gautheryrou, Handbook of soil analysis – mineralogical, organic and inorganic methods, Springer-Verlag Berlin Heidelberg, 2006.
- [31] X. Li, Y. Li, Z. Ye, Preparation of macroporous bead adsorbents based on poly(vinyl alcohol)/chitosan and their adsorption properties for heavy metals from aqueous solution, *Chem. Eng. J.* 178 (2011) 60–68.
- [32] P. Kim, A. Johnson, C.W. Edmunds, M. Radosevich, F. Vogt, T.G. Rials, N. Labbe, Surface functionality and carbon structures in lignocellulosic-derived biochars produced by fast pyrolysis, *Energy Fuels* 25 (2011) 4693–4703.
- [33] S. Kumar, V.A. Loganathan, R.B. Gupta, M.O. Branett, An assessment of U(VI) removal from groundwater using biochar produced from hydrothermal carbonization, *J. Environ. Manage.* 92 (2011) 2504–2512.
- [34] J. Lehmann, S. Joseph, Biochar for Environmental Management: Science & Technology, Earth Scan Publishers, London, 2009.
- [35] P. Huang, D.W. Fuerstenau, The effect of the adsorption of lead and cadmium ions on the interfacial behavior of quartz and talc, *Colloids Surf. A* 177 (2001) 147–156.
- [36] Y.S. Ho, G. McKay, Sorption of dye from aqueous solution by peat, *Chem. Eng. J.* 70 (1998) 115–124.
- [37] S. Ahmed, S. Chughtai, M.A. Keane, The removal of cadmium and lead from aqueous solution by ion exchange with Na-Y zeolite, *Sep. Purif. Technol.* 13 (1998) 57–64.
- [38] Y. Goksungur, S. Uren, U. Guvenc, Biosorption of cadmium and lead ions by ethanol treated waste bakers's yeast biomass, *Bioresour. Technol.* 96 (2005) 103–109.
- [39] D. Tiwari, S.P. Mishra, M. Mishra, R.S. Dubey, Biosorptive behaviour of Mango (*Mangifera indica*) and Neem (*Azadirachta indica*) bark for  $Hg^{2+}$ ,  $Cr^{3+}$  and  $Cd^{2+}$  toxic ions from aqueous solutions: A radiotracer study, *Appl. Radiat. Isot.* 50 (1999) 631–642.
- [40] Z. Reddad, C. Gerente, Y. Andres, P. Le Cloirec, Adsorption of several metal ions onto a low-cost biosorbent: Kinetic and equilibrium studies, *Environ. Sci. Technol.* 36 (2002) 2067–2073.
- [41] A.E. Martell, R.M. Smith, NIST Critically Selected Stability Constants of Metal Complexes, Version 7.0, NIST, Gaithersburg, 2003.